THE AMERICAN MINERALOGIST, VOL. 55, NOVEMBER–DECEMBER, 1970

THE JOIN DIOPSIDE—IRON OXIDE—SILICA AND ITS RELATION TO THE JOIN DIOPSIDE—FORSTERITE—IRON OXIDE—SILICA[1]

RALPH H. NAFZIGER,[2] *The Pennsylvania State University, University Park, Pennsylvania 16802.*

ABSTRACT

Phase relations in the join diopside-iron oxide-silica have been determined at oxygen fugacities corresponding to those associated with basic igneous rocks and defined by a constant room-temperature CO_2/H_2 ratio of 50 under one atmosphere total pressure. A small olivine primary phase field exists, together with three piercing points whose liquid compositions (given in weight percent with iron oxide calculated as Fe_3O_4), temperatures, and oxygen fugacities follow:

(1) 52 $CaMgSi_2O_6$, 40 iron oxide, 8 SiO_2, 1162°C, $\log f_{O_2} = -8.29$, (2) 27 $CaMgSi_2O_6$, 47 iron oxide, 26 SiO_2, 1145°C, $\log f_{O_2} = -8.40$, (3) 17 $CaMgSi_2O_6$, 57 iron oxide, 26 SiO_2, 1173°C, $\log f_{O_2} = -7.97$.

Crystalline phases in equilibrium with liquid are (1) olivine—diopside—magnetite (magnesio-ferrite), (2) olivine—silica—diopside, and (3) olivine—silica—magnetite. One pertinent invariant point (olivine—silica—diopside—magnetite) exists in the system $CaMgSi_2O_6$—FeO—Fe_2O_3—SOi_2. The present data permit qualitative delineation of liquidus phase relations in the petrologically important tetrahedron $CaMgSi_2O_6$—Mg_2SiO_4—iron oxide—SiO_2 at oxygen fugacities defined previously. The sequence of crystallizing phases of simplified ultrabasic magmas is unchanged from that described in the literature at various constant oxygen fugacities.

INTRODUCTION

One tetrahedron which contains the phases olivine, diopside, pyroxene,[3] and magnetite in the system CaO—MgO—FeO—Fe_2O_3—SiO_2 is $CaMgSi_2O_6$—Mg_2SiO_4—iron oxide—SiO_2. Of its four limiting joins, only phase relations in $CaMgSi_2O_6$—iron oxide—SiO_2 have not been explicitly determined previously. In this experimental study, the liquidus and subliquidus phase relations were determined in this join at one atmosphere total pressure and at oxygen fugacities which are applicable to understanding the crystallization of basaltic magmas. Figure 1 illustrates the tetrahedron CaO—MgO—iron oxide—SiO_2 with iron oxide plotted as Fe_3O_4. The included $CaMgSi_2O$—Fe_3O_4—SiO_2 join is sketched therein.

Binary systems do not bound any of the sides of the join $CaMgSi_2O_6$—iron oxide—SiO_2. This is because not all phase compositions represented

[1] Contribution No. 69–52 from College of Earth and Mineral Sciences, The Pennsylvania State University.

[2] Present address: U.S. Bureau of Mines, Albany, Oregon, 97321.

[3] It is recognized that diopside is a pyroxene. Therefore, whenever "pyroxene" is mentioned in this paper as a separate phase, it is taken to mean a calcium-poor or pigeonitic pyroxene.

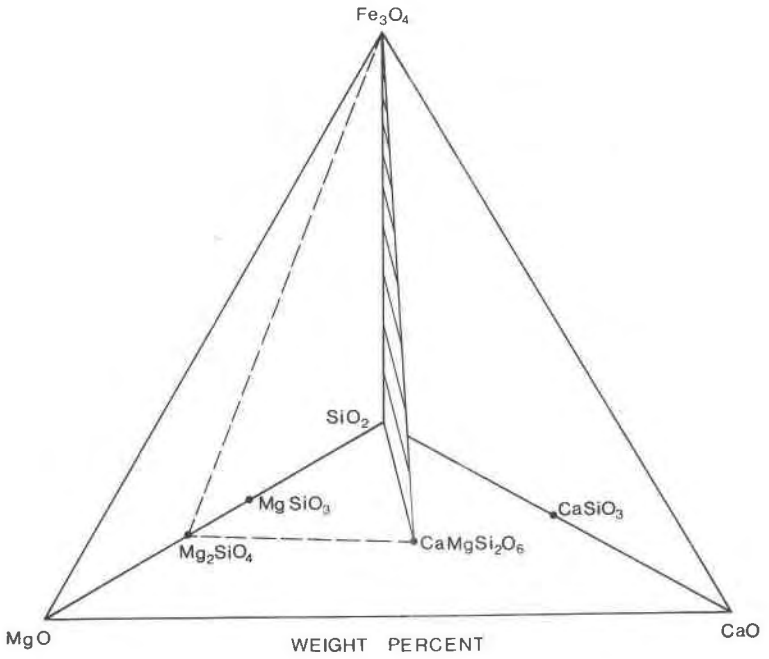

FIG. 1. The tetrahedron CaO—MgO—iron oxide—SiO_2 showing the join $CaMgSi_2O_6$—iron oxide—SiO_2 of the present study as a ruled surface. The dashed lines represent the limits of the join $CaMgSi_2O_6$—Mg_2SiO_4—iron oxide—SiO_2 which is referred to later in this paper. Iron oxide is represented as Fe_3O_4.

within the join can be represented explicitly by the aforementioned end-members. All of the crystalline phases present except tridymite and cristobalite exhibit some cation substitution (for example, CaO and MgO are not always present in each phase in a 1:1 "diopside" ratio). The limiting join $CaMgSi_2O_6$—SiO_2 was determined by Bowen (1914) and later modified by Kushiro and Schairer (1963), and Schairer and Kushiro (1964). The liquidus has a minimum at 1371 ± 1°C and 15–16 weight percent SiO_2 separating the diopside+liquid and tridymite+liquid regions. Phase relations along the join $CaMgSi_2O_6$—iron oxide were studied in air by Presnall (1966). Muan (1955) has made an extensive study of the system FeO—Fe_2O_3—SiO_2 from which data can be obtained for the limiting join iron oxide—SiO_2 at the appropriate gas composition.

EXPERIMENTAL METHOD

Starting materials consisted of the following reagent-grade chemicals which were heat-treated as indicated: Fe_2O_3 at 700°C for 12 hr; MgO at 1400°C for 22 hr; $CaCO_3$ at 300°C for 22 hr; and silicic acid at 400°C for 6 hr, 900°C for 2 hr, and 1350°C for 20 hr. Ten-gram

mixtures in the join $CaMgSi_2O_6$—iron oxide—SiO_2 were prepared from the oxides (see Table 1 for mixture compositions).[1] The ground mixtures were fired in iron-saturated platinum crucibles in air at approximately 800°C for 4 hrs. and then at 1350°C to 1480°C, depending on the estimated liquidus temperature for each mixture, for 15–19 hrs., and quenched. This procedure was repeated until a homogeneous glass was obtained as determined by refractive index measurements. The finely-ground glasses were used as starting materials for all runs on this join.

The now familiar quenching technique (Day, Shepard, and Wright, 1906) was used in the present work. All runs were made in either 55%Ag—45% Pd or 50%Ag—50%Pd crucibles or envelopes to minimize loss of iron to the container (Muan, 1963) at a CO_2/H_2 room-temperature mixing ratio of 50 and quenched in mercury. Run furnaces were of the vertical resistance type whose temperatures were controlled by commercial electronic controllers using Pt/Pt-10%Rh sensing thermocouples. The desired CO_2/H_2 ratio was obtained by mixing chemically-pure grade gases in modified gas mixers of the type used by Darken and Gurry (1945). Gas mixer capillaries were calibrated using a volumetrically calibrated bubble tower. The gas mixture was introduced at the bottom of the furnace by means of a glass quench cup held in place on the furnace by a gas-tight rubber sleeve. The quenching mercury was stored in a reservoir and was introduced into the quench cup only during run quenching. The gas flow rate was that necessary to minimize thermal diffusion and maintain a positive pressure at the top of the furnace. The entire experimental apparatus was periodically calibrated at the FeO—Fe_3O_4 and Fe_3O_4—Fe_2O_3 boundaries at a given temperature. Temperatures were measured before and after each run in an air atmosphere by a Pt/Pt—10%Rh working thermocouple which was frequently calibrated with a standard thermocouple of the same type which in turn was calibrated at the melting point of gold (1062.6°C) and diopside (1391.5°C). Temperatures are believed to be within ± 4°C of the true values.

Phases were identified microscopically in transmitted and/or reflected light. The difficulty in distinguishing between the diopside and olivine phases in the present join was minimized by etching the polished mounts with concentrated HCl (olivine was etched, whereas diopside was not). Phase identification was often verified by X-ray powder diffractometry using Mn-filtered iron radiation. The length of the runs varied from one to three days which was established by preliminary runs as sufficient time to achieve equilibrium.

There are three possible choices of atmosphere in the present type of work: (1) constant CO_2/H_2 mixing ratio, (2) constant oxygen fugacity, or (3) solid buffering (Eugster and Wones, 1962). If this experimental work is to be applicable to basaltic rocks, an oxygen fugacity in the range of 10^{-6} to 10^{-8} atm is probably the correct interval for use with temperatures between 1000°C and 1300°C, based on the work of Fudali (1965) on natural rock samples, and in experimental systems whose phase assemblages are applicable to such rocks (see for example, Muan and Osborn, 1956, Osborn, 1959, 1962, Roeder and Osborn, 1966, Presnall, 1966). A constant oxygen fugacity in the above-mentioned range is generally difficult to achieve with convenient available gases at the relatively low temperatures expected in some parts of the present join. Solid buffers are more difficult to work with experimentally than a constant CO_2/H_2 mixing ratio. A carefully chosen CO_2/H_2 mixing ratio is desirable because its oxygen fugacity can parallel that of several important solid buffer curves. This is illustrated in Figure 2 wherein the mixing ratio chosen for

[1] Table 1 listing results of equilibration runs may be ordered as NAPS Document No. 01111 from National Auxiliary Publications Service of the A.S.I.S., c/o CCM Information Corporation, 909 Third Avenue, New York, N.Y. 10022; remitting $2.00 for microfiche or $5.00 for photocopies, in advance payable to CCMIC NAPS.

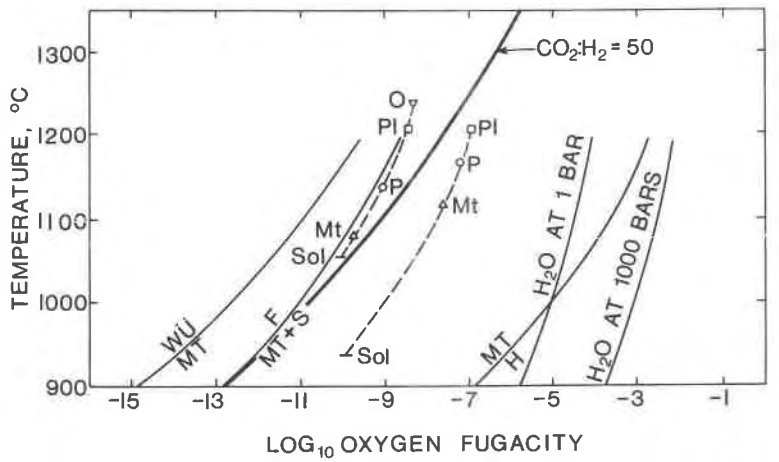

FIG. 2. Temperature-log oxygen fugacity plot showing relations and crystallization sequences involving an olivine basalt (left dashed curve) and a hypersthene-augite andesite (right dashed curve) as sketched by Osborn (1963) from temperature-oxygen fugacity data of Fudali (1965). Light solid lines show three important iron oxide reactions from Eugster and Wones (1962), and two water curves from Kennedy (1948). Superimposed on this diagram of Osborn (1963) are illustrated the temperature-log oxygen fugacity relations of the constant room temperature CO_2/H_2 mixing ratio used in the present study (heavy solid line). Abbreviations are: F-fayalite, H-hematite, Mt-magnetite, O-olivine, Pl-plagioclase, P-pyroxene, S-silica, Sol-solidus, and Wü-wüstite.

this study (50) is plotted on a temperature-log oxygen fugacity diagram which also shows the previously mentioned curves. A CO_2/H_2 ratio of 50 falls in the oxygen fugacity region of basalts and andesites. The two dashed curves for a basalt and an andesite are taken from Osborn (1963), who sketched these curves to show only the general and approximate relations to be expected during equilibrium crystallization in a closed system. Oxygen fugacities for the two rock types at 1200°C and temperatures of appearance of the phases were obtained by Fudali (1965).

EXPERIMENTAL RESULTS

Results of quenching experiments in the join $CaMgSi_2O_6$—iron oxide—SiO_2 are given in Table 1 and are used to construct the liquidus surface shown in Figure 3. All of the iron oxide has been recalculated as Fe_3O_4 and plotted as such in the figure, following the method of Muan and Osborn (1956) with limitations and uses as indicated by Presnall (1966). Thus the phase relations obtained at a constant CO_2/H_2 ratio of 50 in the system $CaMgSi_2O_6$—FeO—Fe_2O_3—SiO_2, which could be represented by a complex surface, have in effect been projected onto the $CaMgSi_2O_6$—Fe_3O_4—SiO_2 plane as shown in Figure 3. Three piercing points are obtained which contain the following crystalline phases in equilibrium with liquid: (1) olivine-diopside-magnesioferrite, (2) olivine-silica—

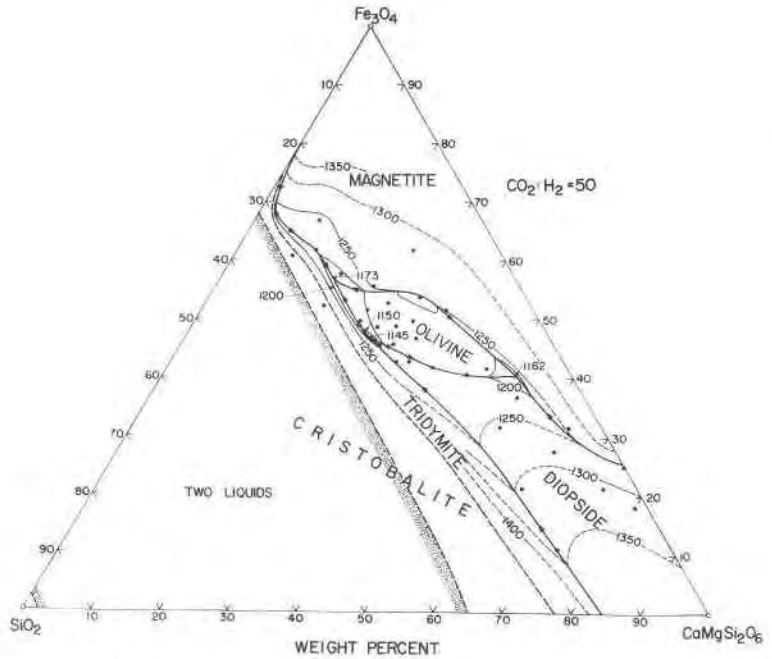

FIG. 3. Liquidus relations in the join $CaMgSi_2O_6$—iron oxide—SiO_2 at a constant room temperature CO_2/H_2 mixing ratio of 50. All iron oxide has been recalculated and plotted as Fe_3O_4. Solid circles represent the compositions of the mixtures studied. Heavy solid lines are liquidus boundary curves (dashed where inferred) and light lines represent liquidus isotherms (solid where known and dashed where inferred). Temperatures are indicated in °C. Arrows on the boundary curves indicate directions of decreasing temperatures. Temperatures of the three piercing points are shown. Stippled areas denote the limits of the liquid immiscibility region

diopside, and (3) olivine—silica—magnesioferrite. Approximate compositions (weight percent), temperatures, and corresponding log oxygen fugacities of these points are: (1) 52 percent $CaMgSi_2O_6$, 40 percent Fe_3O_4, 8 percent SiO_2, 1162°C, −8.29, (2) 27 percent $CaMgSi_2O_6$, 47 percent Fe_3O_4, 26 percent SiO_2, 1145°C, −8.40, and (3) 17 percent $CaMgSi_2O_6$, 57 percent Fe_3O_4, 26 percent SiO_2, 1173°C, −7.97. These three points serve to delineate boundary conditions for the join $CaMgSi_2O_6$—Mg_2SiO_4—iron oxide—SiO_2 at $CO_2/H_2=50$ which must therefore contain the three boundary surfaces involving the crystalline phases mentioned above in addition to liquid and vapor phases.

DISCUSSION

The Quaternary System $CaMgSi_2O_6$—FeO—Fe_2O_3—SiO_2. The $CaMgSi_2O_6$—iron oxide—SiO_2 join may be considered in terms of the quaternary

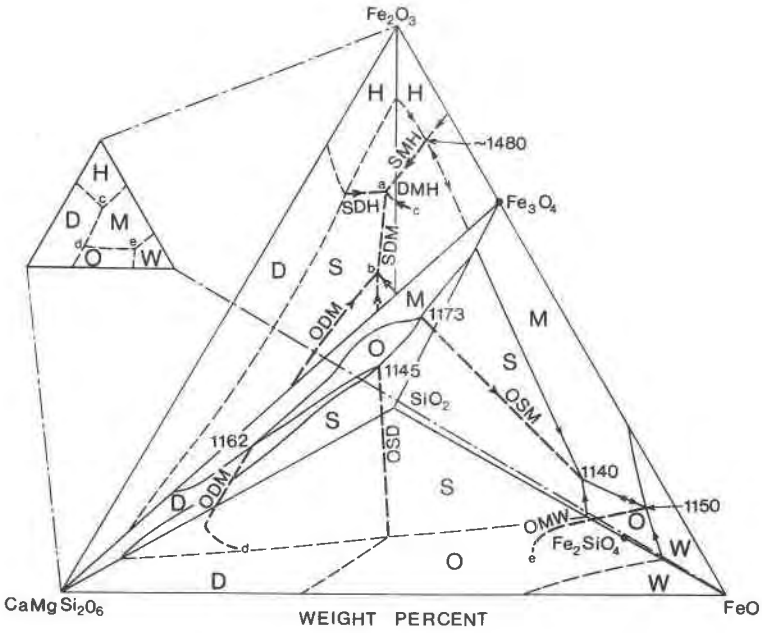

FIG. 4. Schematic weight percent tetrahedron showing phase relations in the system $CaMgSi_2O_6$—FeO—Fe_2O_3—SiO_2 with the SiO_2 apex at the rear. Data on the right face were taken from Muan (1955). The liquidus boundary curves on the base and front face, the latter of which has been removed from the tetrahedron and shown to the left, were partially inferred from the data of Presnall (1966). Phase fields of metallic iron have been omitted for simplicity. The surface $CaMgSi_2O_6$—Fe_3O_4—SiO_2 from Fig. 3 is shown as a plane in this figure. Univariant curves within the tetrahedron are shown as heavy dashed lines and the three crystalline phases in equilibrium with liquid are shown along each. These curves meet at two invariant points within the tetrahedron: a, where silica, diopside, magnesioferrite, and hematite are the equilibrium crystalline phases, and b, where olivine, silica, diopside, and magnesioferrite are such phases. Arrows denote directions of decreasing temperature. Points c, d, and e represent the intersections of univariant curves with the limiting face $CaMgSi_2O_6$—FeO—Fe_2O_3 (front face as represented by the left diagram in the figure). Medium dashed (inferred) or solid lines represent liquidus boundary curves in the limiting faces of the tetrahedron and the plane $CaMgSi_2O_6$—Fe_3O_4—SiO_2. Temperatures are indicated in °C. Abbreviations have the same meaning as in Fig. 2, and D = diopside, M = magnesioferrite, and W = magnesiowüstite. The dot-dashed lines denote projection lines along which the front face has been removed to the left in this figure.

system $CaMgSi_2O_6$—FeO—Fe_2O_6—SiO_2 as shown in Figure 4. From a consideration of the data in the bounding joins (Muan, 1955, Presnall, 1966), four of the three-crystalline phase assemblages which exist along univariant boundary curves in the aforementioned system are olivine—magnesioferrite—magnesiowüstite (OMW), olivine—silica—diopside (OSD), olivine—diopside—magnesioferrite (ODM), and olivine—silica—magnesioferrite (OSM). The latter three join at the invariant point

olivine—silica—diopside—magnesioferrite (point b, Figure 4), an equilibrium phase assemblage which does exist based on the present data (see Table 1). Temperatures along three of the aforementioned univariant boundary curves (OSM, OSD, and ODM, Figure 4) probably decrease from the bounding ternary faces to the invariant point with the exception of the curve OSM which probably possesses a temperature maximum for reasons given later in this paper. The fourth univariant line emanating from this point is silica—diopside—magnesioferrite (SDM). Inasmuch as the $CO_2/H_2 = 50$ join intersects three of the boundary curves at the determined piercing points (see Figure 4), this means that the point olivine—silica—diopside—magnesioferrite lies on the more oxidizing side of the $CO_2/H_2 = 50$ surface in the $CaMgSi_2O_6$—FeO—Fe_2O_3—SiO_2 tetrahedron. Another possible four-phase crystalline assemblage shown in this tetrahedron is silica-diopside-magnesioferrite-hematite (point a, Figure 4).

Relation of Results to the $CaMgSi_2O_6$—Mg_2SiO_4—Iron Oxide—SiO_2 Join. The present data combined with previous work permit delineation of all the important boundary curves wherein two crystalline phases are in equilibrium with liquid at the appropriate gas compositions in the four *limiting faces of the join $CaMgSi_2O_6$—Mg_2SiO_4—iron oxide—SiO_2 which* is shown as an equilateral tetrahedron in Figure 5 with iron oxide plotted as Fe_3O_4. Data for the base ($CaMgSi_2O_6$—Mg_2SiO_4—SiO_2) were taken from Kushiro and Schairer (1963). Curves shown for the Mg_2SiO_4—iron oxide—SiO_2 plane (left face) were obtained by interpolation of constant CO_2/H_2 mixing ratio data presented by Muan and Osborn (1956). Determination of the correct condensed phase assemblages at the piercing points for $CO_2/H_2 = 50$ was made from the log oxygen fugacity-temperature plots of Speidel and Nafziger (1968) for this face. Data from the present work are shown on the right face. Phase relations on the front face (small figure to the left in Figure 5, $CaMgSi_2O_6$—iron oxide—Mg_2SiO_4) at $CO_2/H_2 = 50$ are inferred from the data of Presnall (1966) at an oxygen fugacity of 10^{-6} atm. with total iron recalculated as Fe_3O_4. Three invariant[1] points within the tetrahedron are shown schematically in Figure 5. Two of these [condensed phases: olivine—diopside—pyroxene—magnesioferrite (ODPM), liquid (f in Figure 5), and silica—diopside—pyroxene—magnesioferrite (SDPM), liquid (g in Figure 5)] have previously been postulated by Osborn (1962) and Presnall (1966).

[1] For sake of convenience, boundary curves and their points of intersection within the tetrahedra of Figure 5 and 6 are referred to as "univariant," and invariant," respectively, although these tetrahedra do not represent true quaternary systems for reasons discussed previously in this paper.

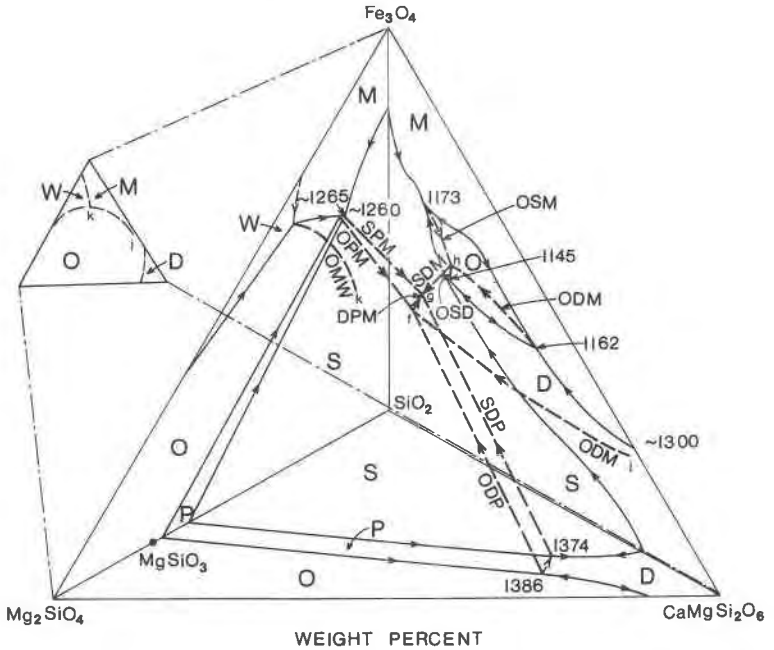

FIG. 5. The join $CaMgSi_2O_6$—Mg_2SiO_4—Fe_3O_4—SiO_2 at $CO_2/H_2 = 50$ with the SiO_2 apex at the rear. Data on the faces of the tetrahedron were obtained as explained in the text. Univariant curves within the tetrahedron are shown as heavy dashed lines which meet at three invariant points: f, where olivine, diopsode, pyroxene, and magnesioferrite are the equilibrium crystalline phases: g, where silica, diopside, pyroxene, and magnesioferrite are such phases; and h, where olivine, silica, diopside, and magnesioferrite coexist together. Points j and k denote piercing points where two univariant curves within the tetrahedron intersect the limiting front face (small diagram at the left). Abbreviations have the same meaning as in Figs. 2 and 4. Temperatures are shown in °C.

Olivine—silica—diopside—magnesioferrite (OSDM), and liquid are the condensed phases present at the third proposed point (h in Figure 5). The existence of this point is postulated on the basis of results shown in Table 1 (mixtures 16, 25, 40, and 41). The maximum temperature range for this point lies between 1091°C and 1144°C at corresponding log oxygen fugacities of −9.18 and −8.43.

The present work verifies the existence of an olivine primary phase field in the join $CaMgSi_2O_6$—iron oxide—SiO_2 at oxygen fugacities defined by a room-temperature CO_2/H_2 mixing ratio of 50 and the consequent delineation of invariant points in this join. At lower oxygen fugacities, the olivine field would be expected to increase in size at the expense of the magnesioferrite until the latter disappears entirely, thus eliminating the piercing points which include magnesioferrite as a stable

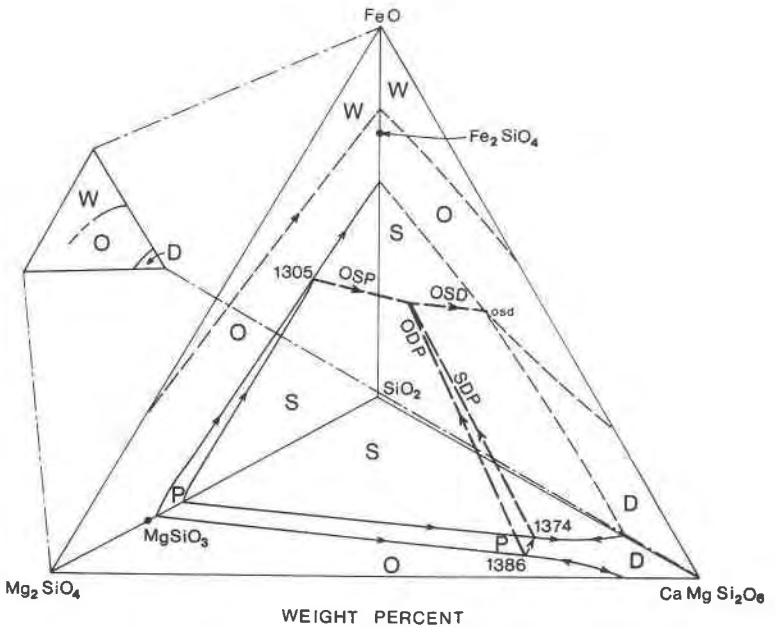

FIG. 6. Inferred phase relations in the join $CaMgSi_2O_6$—Mg_2SiO_4—iron oxide—SiO_2. Crystalline phases are in equilibrium with liquid and metallic iron. All iron oxide is plotted as FeO. The data on the left face of the tetrahedron are from Bowen and Schairer (1935), those on the front face (here shown removed from the tetrahedron and placed to its left) from Presnall (1966), and those on the right face from Ricker (1952). Curves and symbols have the same meaning as in Figs. 4 and 5. One invariant point within the tetrahedron is indicated where olivine, silica, diopside, and pyroxene are in equilibrium with liquid and a gas phase whose oxygen fugacity is that defined in equilibrium with metallic iron. Primary phase fields of metallic iron have been omitted

phase. This supposition is based on phase relations as a function of oxygen fugacity which obtain in analogous systems involving iron oxide, silica, and/or calcium and/or magnesium silicate (see for example, Muan and Osborn, 1956, Presnall, 1966, Speidel and Nafziger, 1968). A magnesiowüstite field appears and the inferred relations in equilibrium with metallic iron are shown as the right face of the tetrahedron in Figure 6. Only one piercing point (osd)[1] is shown in this face and the number of invariant points and univariant curves within the tetrahedron are reduced, resulting in the more simple relations shown in Figure 6.

Crystallization Sequences. Using the relations shown in Figure 5, qualitative fractional crystallization sequences for mixtures at oxygen fugacities

[1] The lower case letters refer to crystalline phases coexisting in equilibrium in the bounding joins of the tetrahedron, following the notation of Speidel and Nafziger (1968).

obtained from a fixed room-temperature CO_2/H_2 ratio of 50 can be derived. At this constant CO_2/H_2 ratio, the oxygen fugacity will continuously decrease as cooling progresses, but at a slower rate than that which obtains in a closed system [*i.e.* crystallization at a constant composition (see for example, Osborn, 1969)]. When $CO_2/H_2 = 50$, there is still a sufficient magnesioferrite volume to prevent the crystallizing liquid from moving to compositions high in iron oxide relative to silica. The fractional crystallization of mixtures lying within the tetrahedron of Figure 5 would result in phase sequences very similar to those described by Osborn (1962) and Presnall (1966) at constant oxygen fugacities. The present data also characterize more specifically the relations along the curve SDM in Figure 5 (curve DE in Osborn, 1962, Figure 4, and the curve originating at e, e′, and e″ in Presnall, 1966, Figure 6). Mixtures whose bulk compositions lie within the small olivine volume in the right of the tetrahedron in Figure 5 would crystallize in the sequence: olivine; olivine+magnesioferrite, or olivine+diopside; olivine+silica+magnesioferrite, olivine+diopside+magnesioferrite, or olivine+silica+diopside. The precise sequence will depend on the bulk compositions and the changing compositions of the crystallizing phases. In any case, all of these mixtures would crystallize toward point h (OSDM) in Figure 5. Mixtures whose bulk compositions lie near the $CaMgSi_2O_6$—Fe_3O_4—SiO_2 plane in the vicinity of the olivine volume would crystallize in a similar manner as outlined above.

ACKNOWLEDGMENTS

This work received support from the National Science Foundation, Grant GA-459. The author wishes to thank Prof. E. F. Osborn for helpful counsel during the course of this research and for suggesting improvements in the manuscript.

REFERENCES

BOWEN, N. L. (1914) The ternary system diopside—forsterite—silica. *Amer. J. Sci.* **188,** 207–264.

——— AND J.F. SCHAIRER (1935) The system MgO—FeO—SiO_2. *Amer. J. Sci.* **229,** 151–217.

DARKEN, L. S. AND R. W. GURRY (1945) The system iron-oxygen. I. The wüstite field and related equilibria. *J. Amer. Chem. Soc.* **67,** 1398–1412.

DAY, A. L., E. S. SHEPARD, AND F. E. WRIGHT (1906) The lime-silica series of minerals. *Amer. J. Sci.* **172,** 265–302.

EUGSTER, H. P. AND D. R. WONES (1962) Stability relations of the ferruginous biotite, annite. *J. Petrology,* **3,** 82–125.

FUDALI, R. F. (1965) Oxygen fugacities of basaltic and andesitic magmas. *Geochim. Cosmochim. Acta,* **29,** 1063–1075.

KENNEDY, G. C. (1948) Equilibrium between volatiles and iron oxides in igneous rocks. *Amer. J. Sci.* **246,** 529–549.

KUSHIRO, I., AND J. F. SCHAIRER (1963) New data on the system diopside—forsterite—silica. *Carnegie Inst. Wash. Year Book,* **62,** 95–103.

MUAN, A. (1955) Phase equilibria in the system FeO—Fe_2O_3—SiO_2. *J. Metals*, **203**, 965–976.

——— (1963) Silver-palladium alloys as crucible material in studies of low-melting iron silicates. *Amer. Ceram. Soc. Bull*, **42**, 344–347.

———, AND E. F. OSBORN (1956) Phase equilibria at liquidus temperatures in the system MgO—FeO—Fe_2O_3—SiO_2. *J. Amer. Ceram. Soc.* **39**, 121–140.

OSBORN, E. F. (1959) Role of oxygen pressure in the crystallization and differentiation of basaltic magmas. *Amer. J. Sci.* **257**, 609–647.

——— (1962) Reaction series for subalkaline igneous rocks based on different oxygen pressure conditions. *Amer. Mineral.* **47**, 211–226.

——— (1963) Some experimental investigations bearing on the origin of igneous magmas of the earth's crust. *Inst. Invest. Geol. Lucas Mallada Estud. Geol. (Madrid)*, **19**, 1–7.

——— (1969) Experimental aspects of calc-alkaline differentiation. *Bull. Ore. Dep. Geol. Miner. Ind.* **65**, 33–42.

PRESNALL, D. C. (1966) The join forsterite-diopside-iron oxide and its bearing on the crystallization of basaltic and ultramafic magmas. *Amer. J. Sci.* **264**, 753–809.

RICKER, R. W. (1952) *Phase Equilibria in the Quaternary System CaO—MgO—FeO—SiO_2.* Ph.D. thesis, The Pennsylvania State University.

ROEDER, P. L., AND E. F. OSBORN (1966) Experimental data for the system MgO-FeO-Fe_2O_3—$CaAl_2Si_2O_6$—SiO_2 and their petrologic implications. *Amer. J. Sci.* **264**, 428–480.

SCHAIRER, J. F., AND I. KUSHIRO (1964) The join diopside-silica. *Carnegie Inst. Wash. Year Book*, **63**, 130–132.

SPEIDEL, D. H. AND R. H. NAFZIGER (1968) P-T-f_{O_2} relations in the system Fe-O-MgO-SiO_2. *Amer. J. Sci.* **266**, 361–379.

Manuscript received, May 13, 1970; accepted for publication, June 3, 1970.